OSCILLATORY THERMOCONVECTIVE INSTABILITY IN A VISCOELASTIC MAGNETIC FLUID SATURATED ANISOTROPIC POROUS MEDIUM WITH SECOND SOUND

Naseer Ahmed[1*], S Maruthamanikandan[2]

Article History: Received: 01.04.2023 **Revised:** 05.05.2023 **Accepted:** 24.06.2023

Abstract

The classical stability analysis is used to examine the combined effect of viscoelasticity, thermal and mechanical anisotropic effects on the onset of porous medium ferroconvection. The fluid and solid matrix are assumed to be in local thermal equilibrium. Considering the boundary conditions appropriate for an analytical approach, the critical values pertaining to both stationary and oscillatory instabilities are obtained by means of the normal mode analysis. It is delineated that oscillatory instability is preferred to stationary instability depending on the range of various parameters. It is also shown that oscillatory porous medium ferroconvection is advanced through the magnetic forces, nonlinearity in magnetization, stress relaxation due to viscoelasticity and the mechanical anisotropy. On the other hand, it is observed that the presence of the stress retardation and the thermal anisotropy delay the onset of oscillatory porous medium ferroconvection. The effect of various parameters on the size of the convection cell is also discussed. The results of the problem may have possible implications for engineering and technological applications wherein magnetic fluids are encompassed along with the viscoelastic and anisotropic properties.

Keywords: Convection, Maxwell equations, Viscoelastic fluids, Porous media, Navier-Stokes equations, magnetic fluids, Anisotropy.

PACS: 46.25.Hf, 47.55.P-, 77.84.Nh, 41.20.-q, 77.22.-d

[1*]Department of Mathematics, Presidency College, Kempapura, Hebbal, Bengaluru - 560024, India
Email: [1*]naseerahmed.ar2023@gmail.com
ORCID ID: [1*]https://orcid.org/0000-0002-5327-9362
[2]Department of Mathematics, School of Engineering, Presidency University, Bengaluru - 560064, India
Email: [2]maruthamanikandan@presidencyuniversity.in
ORCID ID: [2]https://orcid.org/0000-0001-9811-0117

***Corresponding Author:**
Naseer Ahmed[1*]
[1*]Department of Mathematics, Presidency College, Kempapura, Hebbal, Bengaluru - 560024, India
Email: [1*]naseerahmed.ar2023@gmail.com
ORCID ID: [1*]https://orcid.org/0000-0002-5327-9362

DOI: 10.31838/ecb/2023.12.6.83

1. INTRODUCTION

Magnetic particles are a class of micrometre-sized particles that respond to an applied magnetic field. Depending on their behaviour they are classified into five types: ferromagnetic, anti-ferromagnetic, paramagnetic, ferrimagnetic and diamagnetic. Due to unpaired electrons, an atom will have a net magnetic moment in ferromagnetic materials and a giant net magnetic moment is formed in the presence of a magnetic field. Materials belonging to the ferromagnetic particles' family are nickel, iron, and cobalt. A carrier fluid in which well-dispersed ferromagnetic particles are present is called a ferrofluid (or a ferromagnetic fluid). The agglomeration tendency in the suspended particles of ferromagnetic in a carrier fluid is avoided by coating these particles with a surfactant like soy lecithin, oleic acid, and citric acid. Due to this coating, the ferrofluids turn into eminently stable and will have vigorous magnetic properties. Ferromagnetic fluids have numerous applications in various fields. Transporting of drugs to damaged part of the body and tumours discharge from the body in medical field are a couple of the practical usage of ferromagnetic fluids. Ferrofluids also find their applications in loudspeakers, coolants, rotating shafts, seals, semi-active dampers, printers and aerospace related areas. As for the heat transfer applications, thermal conductivity enhancement is observed in carrier fluids, which leads to enhanced heat transport, due to the existence of ferromagnetic particles.

Ferrofluids are known as "smart fluids" because their rheological dynamics can be restrained by an external applied magnetic field [1]. Rosensweig [2] coined the prefix "ferro" and was the first to synthesize a ferrofluid. An exhaustive linear stability analysis of Rayleigh-Bénard convection (RBC) in a ferrofluid was examined by Finlayson [3] by taking account of both magnetic and buoyancy mechanisms. After this work, Schwab et al. [4] examined the results of Finlayson [3] theoretically, whereas Stiles and Kagan [5] did them experimentally. Lalas and Carmi [6] reported the unique results concerning stationary ferromagnetic convection with energy stability analysis. Bajaj and Malik [7, 8] worked on the pattern formation in a ferrofluid and concluded that compared to the hexagonal and square lattices, rolls are more stable. Maruthamanikandan [9] analysed the effect of radiative transfer on the onset of thermal convection in a ferromagnetic fluid layer confined between two parallel plates and heated from below. The Milne-Eddington approximation is employed to convert radiative heat flux into thermal heat flux. The opaque medium is shown to release heat for ferroconvection more slowly than the transparent medium. Outcome of comparison of critical values based on the energy stability analysis with those of linear and weakly nonlinear stability analyses was considered by Straughan [10]. Several other fascinating studies have been performed to investigate thermomagnetic convection in a ferrofluid layer with a variety of geometries and physical mechanisms [11 - 18].

The thermal convection study in porous media, a frequent instance in nature with a vast scope of technological applications, appears to have developed as a result of the flow's resemblance to the classical Rayleigh-Bènard convection. From a phenomenological perspective, these two actually have a lot in common. Following the innovative work of Horton and Rogers [19] and Lapwood [20], there has been a significant amount of effort in the subject matter concerning convective instability of a variety of fluids in porous media. Malashetty and Padmavathi [21] investigated the effect of gravity modulation on the onset of convection in a porous layer with an apparent viscosity greater than the fluid viscosity. Govender [22] explored empirically the influence of universal gravitation on centrifugally propelled advection in a rotating porous matrix separated from the axis of rotation. El Sayed [23] investigated the commencement of electrohydrodynamic destabilization in an Oldroyd viscoelastic liquid electrolyte through a sparsely permeable media under the combined effects of a perpendicular alternating electrical current and a perpendicular temperature gradient. Advection commencement in a nanofluid layer saturated by a permeable structure was reported by Kuznetsov and Nield [24]. Eltayeb [25] examined the steadiness of a permeable Benard-Brinkman liquid flow in a material under heat transfer coefficients and quasi

regimes. Soya and Maruthamanikandan [26] implemented the technique of small disturbance to study the variable viscosity impact on Darcy-Brinkman ferroconvection by assuming the effective viscosity as temperature dependent. Saravanan and Meenasaranya [27] used a dynamical technique to investigate the free convective onset in a bottom warmed permeable medium confined to a cross-sectional magnetic field. Castinel and Combarnous [28] was the first to study natural convection in a fluid layer filled with anisotropic permeable structure. Many other studies have been conducted to investigate convection in a fluid layer filled by anisotropic permeable medium [29 - 37].

The temperature's governing equation (heat transport equation) in classical theory accepts a partial differential equation of parabolic type that permits thermal signals at an infinite speed, which is impractical. As a result, classical Fourier's law of heat conduction is modified by new theories to encompass a hyperbolic type of heat transport equation that introduces thermal signals at a non-infinite speed. As per this theory, heat propagates as a wave phenomenon instead of a diffusion phenomenon and the wavelike thermal disturbance is referred to as second sound. Straughan and Franchi [38] were the first to research the propagation of thermal waves upon the onset of convective instability and the results from their analysis were significantly different from the classical case. They concluded that oscillatory convection occurs only for values of the Cattaneo number above a threshold value and that the stability of a Maxwell-Cattaneo fluid in Bénard problem is always less than that of the classical one. Straughan [39] adopted the heat flux law of Cattaneo to investigate thermal convection for a layer of fluid in the light of findings concerning the second sound. Soya and Maruthamanikandan [40] studied the porous medium ferromagnetic instability with the heat conduction law due to Maxwell-Cattaneo. Recently, Vidya Shree et al. [41] investigated the combined effect of MFD viscosity and second sound on the onset of Darcy-Brinkman ferroconvection.

Due to the implications of Rayleigh-Bénard convection (RBC) problems concerning Newtonian liquids for heat transfer and alternative engineering utilization ([42], [43] and references therein) has received a widespread attention. But all liquids are not Newtonian liquids. In the present paper, we are concerned with one such liquid called a viscoelastic liquid. Polymeric liquids, gel-based fluids and DNA suspensions are examples of viscoelastic liquids. This liquids exhibit both liquid and solid properties and hence throw light on various applications in petroleum, chemical and nuclear industries. A vital role is played by these liquids in material processing, geothermal energy modelling, thermal insulation materials, transport of chemical substances, cooling of electronic devices, injection moulding, crystal growth and solar receivers. Usually there are one or two relaxation times in the rheological equation for viscoelastic liquids and a good discussion on this aspect is available in books ([44], [45] and references therein). Oldroyd model [46] gives the simplest rheological equation that describes realistically the viscoelastic properties of diluted polymers such as water solutions or Boyer liquids of polyacrylamides. The examination of the RBC problem in viscoelastic liquids is vital since it can assist as a rheometric tool for the analysis of viscosity which is otherwise challenging in the case of such liquids. Vest and Arpaci [47] reported the rigid boundaries effect in a Maxwellian liquid. They showed that the elasticity destabilizes the system and due to the effect of rigid boundaries stability advances slightly when compared to the case of the stress-free boundaries. Liang and Acrivos [48] by experimental observation conveyed that the Nusselt number, quantifying the heat transport, at any given Rayleigh number is marginally but frequently higher for a viscoelastic liquid than that of a Newtonian liquid of proportionate viscosity. Shenoy and Mashelkar [49] reported the influence of viscoelastic effects on the onset of convection and the heat transport. Martinez-Mardones et al. [50] reported the thermal convection influencing binary liquid of polymeric solution. Several other control effects on the convection dynamics in viscoelastic fluids have been well documented in a number of investigations [51 – 60].

Keeping in mind the aforementioned literature review, the present study is devoted to

investigating the problem of anisotropic porous medium convective instability in a Cattaneo-viscoelastic-ferromagnetic fluid with the intention of exploring the meaningful and possible range of parameters that could lead to oscillatory porous medium viscoelastic ferroconvection.

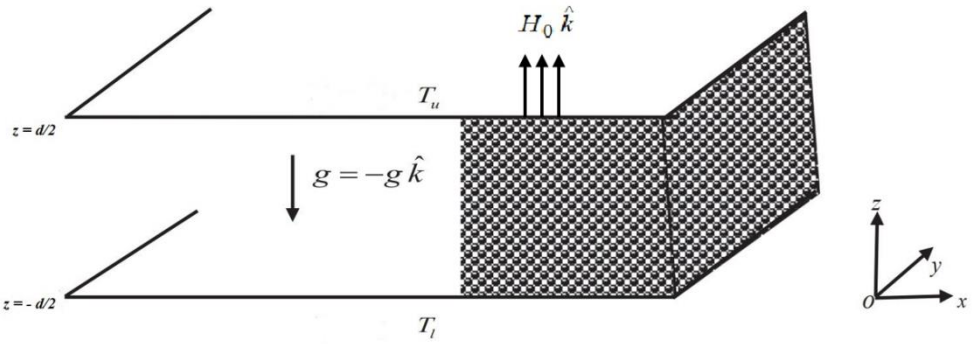

Figure 1. Physical Configuration

2. MATHEMATICAL FORMULATION

Let us consider an incompressible Cattaneo-viscoelastic-ferromagnetic fluid situated between the two surfaces of non-finite length horizontally of finite thickness *d*. We consider the Oldroyd's model through an anisotropic porous medium to characterize the viscoelastic behaviour and we assume that the porous layer possesses horizontal isotropy in both mechanical and thermal properties. The lower surface at $z=-\frac{d}{2}$ and upper surface at $z=\frac{d}{2}$ are maintained at temperatures T_l and T_u respectively, where $T_l > T_u$ with $\Delta T = T_l - T_u$ (see Figure 1). It is assumed that at quiescent state the temperature varies linearly across the depth. When the magnitude of ΔT becomes larger than the critical one, thermal convection will set in due to the buoyancy and magnetic forces.

The fluid layer is exposed to a magnetic field $\vec{H}_0$ acting parallel to the vertical *z*-axis and the gravity force acting vertically downwards. We assume that the Oldroyd's model is sufficient to characterize the viscoelastic behaviour which is simple enough to be tractable analytically. The governing equations under the Boussinesq approximation are written

$$\nabla \bullet \vec{q} = 0 \tag{2.1}$$

$$\left(1+\lambda_1\frac{\partial}{\partial t}\right)\left[\frac{\rho_0}{\varepsilon}\frac{\partial \vec{q}}{\partial t}+\frac{\rho_0}{\varepsilon^2}\left(\vec{q}\bullet\nabla\right)\vec{q}+\nabla p-\rho\vec{g}-\nabla\bullet\left(\vec{H}\,\vec{B}\right)\right]$$

$$=\left(1+\lambda_2\frac{\partial}{\partial t}\right)\left[-\mu_f\,\vec{K}\bullet\vec{q}+\overline{\mu_f}\,\nabla^2\vec{q}\right] \tag{2.2}$$

$$\varepsilon\left[\rho_0\, C_{V,H} - \mu_0 \vec{H}\bullet\left(\frac{\partial \vec{M}}{\partial T}\right)_{V,H}\right]\left[\frac{\partial T}{\partial t} + \vec{q}\bullet\nabla T\right] + (1-\varepsilon)\left(\rho_0\, C\right)_s \frac{\partial T}{\partial t} + \mu_0\, T\left(\frac{\partial \vec{M}}{\partial T}\right)_{V,H}\bullet\left[\frac{\partial \vec{H}}{\partial t} + \left(\vec{q}\bullet\nabla\right)\vec{H}\right] = -\nabla\bullet\vec{Q} \tag{2.3}$$

$$\tau\left[\frac{\partial \vec{Q}}{\partial t} + \left(\vec{q}\bullet\nabla\right)\vec{Q} + \vec{\omega}\times\vec{Q}\right] = -\vec{Q} - \left(\vec{K_T}\bullet\nabla T\right) \tag{2.4}$$

$$\rho = \rho_0\left[1 - \alpha\left(T - T_a\right)\right] \tag{2.5}$$

$$M = M_0 + \chi_m\left(H - H_0\right) - K_m\left(T - T_a\right) \tag{2.6}$$

where λ_1 is the stress relaxation time, λ_2 is the strain retardation time $\left(0 \le \lambda_2 < \lambda_1\right)$, $\vec{q}$ = (*u*, *v*, *w*) is the fluid velocity, ρ_0 is the reference density, ε is the porosity, *t* is the time, *p* is the pressure, $\vec{g}$ is the acceleration due to gravity, ρ is the fluid density, μ_f is the dynamic viscosity, $\overline{\mu_f}$ is the effective viscosity, k is the permeability of the porous medium, $\vec{H}$ is the magnetic field, $\vec{B}$ is the magnetic induction, *T* is the temperature, μ_0 is the magnetic permeability, $\vec{M}$ is the magnetization, k_1 is the thermal conductivity, α is the thermal expansion coefficient, $C_{V,H}$ is the specific heat at constant volume and magnetic field, χ_m is the magnetic susceptibility, K_m is the pyromagnetic coefficient, $\vec{Q}$ is the heat flux and τ is a constant with the dimensions of time. Further, $\vec{K} = K_x^{-1}\left(\hat{i}\,\hat{i} + \hat{j}\,\hat{j}\right) + K_z^{-1}\left(\hat{k}\,\hat{k}\right)$ is the anisotropic permeability tensor, $\vec{K_T} = K_{Tx}\left(\hat{i}\,\hat{i} + \hat{j}\,\hat{j}\right) + K_{Tz}\left(\hat{k}\,\hat{k}\right)$ is the anisotropic thermal conductivity tensor and $\vec{\omega} = \frac{1}{2}\nabla\times\vec{q}$.

Maxwell's equations applicable to the problem under consideration are

$$\nabla \bullet \vec{B} = 0, \quad \nabla \times \vec{H} = \vec{0}, \quad \vec{B} = \mu_0 \left(\vec{H} + \vec{M} \right). \tag{2.7}$$

One can have following observation about Oldroyd's fluid. If $\lambda_2 = 0$, the fluid represents the Maxwell's fluid and if both $\lambda_1 = 0$ and $\lambda_2 = 0$, then the fluid signifies the Newtonian fluid. Equations characterizing the basic state are introduced in the form

$$\left.\begin{array}{l} \dfrac{\partial}{\partial t} = 0,\ \vec{q_b} = (0,0,0),\ T = T_b(z), \\ p = p_b(z),\ \rho = \rho_b(z),\ \vec{H} = H_b(z), \\ \vec{M} = M_b(z),\ \vec{B} = B_b(z),\ \vec{Q} = \vec{Q}_b(0,\ 0,\ K_{Tz}\beta) \end{array}\right\} \tag{2.8}$$

where $\beta = \dfrac{T_1 - T_0}{2}$. The solution pertaining to the basic state reads

$$\rho_b = \rho_0 [1 + \alpha \beta z] \tag{2.9}$$

$$\vec{H_b} = \left[H_0 - \frac{K_m \beta z}{1 + \chi_m} \right] \hat{k} \tag{2.10}$$

$$\vec{M_b} = \left[M_0 + \frac{K_m \beta z}{1 + \chi_m} \right] \hat{k} \tag{2.11}$$

$$\vec{B} = \mu_0 \left[\vec{H} + \vec{M} \right] \hat{k} \tag{2.12}$$

3. STABILITY ANALYSIS

We shall obtain the dimensionless equations by embracing the classical stability analysis based on small perturbations and encompassing normal modes (Finlayson [3] and Soya Mathew & Maruthamanikandan [26]). The perturbed state equations involving infinitesimally small perturbations are

$$\left.\begin{array}{l} \vec{q} = \vec{q_b} + \vec{q}',\ T = T_b + T',\ p = p_b + p', \\ \rho = \rho_b + \rho',\ \vec{H} = \vec{H_b} + \vec{H}',\ \vec{M} = \vec{M_b} + \vec{M}', \\ \vec{B} = \vec{B_b} + \vec{B}',\ \vec{Q} = \vec{Q_b} + \vec{Q}',\ \phi = \varphi_b + \phi' \end{array}\right\} \tag{3.1}$$

where the primes indicate the perturbed quantities. The linearized equations involving the small perturbations therefore take the from

$$\left(1+\lambda_1\frac{\partial}{\partial t}\right)\left[\frac{\rho_0}{\varepsilon}\frac{\partial}{\partial t}\left(\nabla^2 w'\right)-\alpha g\rho_0\nabla_1^2 T+\mu_0 K_m\beta\frac{\partial}{\partial z}\left(\nabla_1^2\phi'\right)-\frac{\mu_0 K_m^2\beta\nabla_1^2 T'}{1+\chi_m}\right] =\left(1+\lambda_2\frac{\partial}{\partial t}\right)\left[-\frac{\mu_f}{K_z}\left\{\nabla_1^2+\frac{1}{\xi}\frac{\partial^2}{\partial z^2}\right\}w'+\overline{\mu_f}\,\nabla^4 w'\right] \tag{3.2}$$

$$(\rho_0 C)_1\frac{\partial T'}{\partial t}-\mu_0 T_a K_m\frac{\partial}{\partial t}\left(\frac{\partial\phi'}{\partial z}\right)=-\nabla.\vec{Q}'+\left[(\rho_0 C)_2-\frac{\mu_0 T_a K_m^2}{1+\chi_m}\right]\beta w' \tag{3.3}$$

$$\left(1+\tau\frac{\partial}{\partial t}\right)\vec{Q}'=-\frac{\tau K_{Tz}\beta}{2}\left(\frac{\partial\vec{q}'}{\partial z}-\nabla w'\right)-\left[K_{Tx}\frac{\partial T'}{\partial x}\hat{i}+K_{Tx}\frac{\partial T'}{\partial y}\hat{j}+K_{Tz}\frac{\partial T'}{\partial z}\hat{k}\right] \tag{3.4}$$

$$(1+\chi_m)\frac{\partial^2\phi'}{\partial z^2}+\left(1+\frac{M_0}{H_0}\right)\nabla_1^2\phi'-K_m\frac{\partial T'}{\partial z}=0 \tag{3.5}$$

where $\xi=\dfrac{K_x}{K_z}$ is the mechanical anisotropy parameter. We take divergence on both sides of equation (3.4) and substitute the result in equation (3.3) to eliminate $\vec{Q}'$ from equation (3.3). The new system of linearized perturbed equations turn out to be

$$\left(1+\lambda_1\frac{\partial}{\partial t}\right)\left[\frac{\rho_0}{\varepsilon}\frac{\partial}{\partial t}\left(\nabla^2 w'\right)-\alpha g\rho_0\nabla_1^2 T+\mu_0 K_m\beta\frac{\partial}{\partial z}\left(\nabla_1^2\phi'\right)-\frac{\mu_0 K_m^2\beta\nabla_1^2 T'}{1+\chi_m}\right] =\left(1+\lambda_2\frac{\partial}{\partial t}\right)\left[-\frac{\mu_f}{K_z}\left\{\nabla_1^2+\frac{1}{\xi}\frac{\partial^2}{\partial z^2}\right\}w'+\overline{\mu_f}\,\nabla^4 w'\right] \tag{3.6}$$

$$\left(1+\tau\frac{\partial}{\partial t}\right)\left[(\rho_0 C)_1\frac{\partial T'}{\partial t}-\mu_0 T_a K_m\frac{\partial}{\partial t}\left(\frac{\partial\phi'}{\partial z}\right)\right]-\left[(\rho_0 C)_2-\frac{\mu_0 T_a K_m^2}{1+\chi_m}\right]\beta w' =-\frac{\tau K_{Tz}\beta}{2}\nabla^2 w'+K_{Tz}\left[\eta\nabla_1^2 T'+\frac{\partial^2 T'}{\partial z^2}\right] \tag{3.7}$$

$$\left(1+\chi_m\right)\frac{\partial^2\phi'}{\partial z^2}+\left(1+\frac{M_0}{H_0}\right)\nabla_1^2\,\phi'-K_m\,\frac{\partial T'}{\partial z}=0 \tag{3.8}$$

where $\eta=\frac{K_{Tx}}{K_{Tz}}$ is the thermal anisotropy parameter and ϕ' is the magnetic potential. Further, $\left(\rho_0 C\right)_1=\varepsilon\rho_0 C_{V,H}+\varepsilon\mu_0 H_0 K_m+\left(1-\varepsilon\right)\left(\rho_0 C\right)_s$, $\left(\rho_0 C\right)_2=\varepsilon\rho_0 C_{V,H}+\varepsilon\mu_0 H_0 K_m$,

$\nabla_1^2=\frac{\partial^2}{\partial x^2}+\frac{\partial^2}{\partial y^2}$, $\nabla^2=\nabla_1^2+\frac{\partial^2}{\partial z^2}$, $K_m=-\left(\frac{\partial M}{\partial t}\right)_{V,H}$ and $\chi_m=\left(\frac{\partial M}{\partial H}\right)_{H_o,T_a}$.

The normal mode solution is adopted and the same has the form

$$\begin{bmatrix} w' \\ T' \\ \phi' \end{bmatrix}=\begin{bmatrix} W(z) \\ \Theta(z) \\ \Phi(z) \end{bmatrix}e^{i\left(l\,x+m\,y\right)+\sigma t} \tag{3.9}$$

where *l* and *m* are respectively the wave numbers in the *x* and *y* directions and σ is the growth rate. Substitution of (3.9) into (3.6) to (3.8) leads to

$$\begin{aligned}&\left(1+\lambda_1\sigma\right)\left[\frac{\rho_0}{\varepsilon}\sigma\left(D^2-K_h^2\right)W+\alpha\rho_0 g K_h^2\Theta-\mu_0 K_m\beta K_h^2\,D\Phi\ +\frac{\mu_0 K_m^2\beta K_h^2\,\Theta}{1+\chi_m}\right]\\&=\left(1+\lambda_2\sigma\right)\left[-\frac{\mu_f}{k}\left(\frac{1}{\xi}D^2-K_h^2\right)W+\overline{\mu_f}\left(D^2-K_h^2\right)^2 W\right]\end{aligned} \tag{3.10}$$

$$\begin{aligned}&\left(1+\tau\sigma\right)\left[\left(\rho_0 C\right)_1\sigma\Theta-\mu_0 T_a K_m\,\sigma D\Phi\right]-\left[\left(\rho_0 C\right)_2-\frac{\mu_0 T_a K_m^2}{1+\chi_m}\right]\beta W\\&=-\frac{\tau K_{Tz}\beta}{2}\left(D^2-K_h^2\right)W+K_{Tz}\left(D^2-\eta\,K_h^2\right)\Theta\end{aligned} \tag{3.11}$$

$$\left(1+\chi_m\right)D^2\Phi-\left(1+\frac{M_0}{H_0}\right)K_h^2\,\Phi\left(z\right)-K_m\,D\Theta=0 \tag{3.12}$$

where $D=\frac{d}{dz}$ and $K_h^2=l^2+m^2$ is the overall horizontal wave number.

Non-dimensionalizing equations (3.10) - (3.12) using the scaling

$$\left.\begin{aligned} W^* = \frac{Wd}{\kappa},\ \Theta^* = \frac{\Theta}{\beta d},\ \Phi^* = \frac{\Phi}{\frac{K_m \beta d^2}{1+\chi_m}}, \\ a = K_h d,\ \ z^* = \frac{z}{d},\ \ \sigma^* = \frac{\sigma}{\frac{\kappa}{d^2}} \end{aligned}\right\} \tag{3.13}$$

We obtain

$$\begin{aligned} &\left(1+F_1\,\sigma\right)\left[\frac{\sigma}{\mathrm{Pr}}\left(D^2-a^2\right)W+\left(R+N\right)a^2\,\Theta-N\,a^2\,D\Phi\right] \\ &=\left(1+F_2\,\sigma\right)\left[-Da^{-1}\left(\frac{1}{\xi}D^2-a^2\right)W+\Lambda\left(D^2-a^2\right)^2 W\right] \end{aligned} \tag{3.14}$$

$$\left(1+2G\sigma\right)\left(\lambda\sigma\Theta-M_2\,\sigma D\Phi-\left(1-M_2\right)W\right)=\left(D^2-\eta a^2\right)\Theta-G\left(D^2-a^2\right)W \tag{3.15}$$

$$\left(D^2-M_3\,a^2\right)\Phi-D\Theta=0 \tag{3.16}$$

where $\lambda=\frac{\left(\rho_0 C\right)_1}{\left(\rho_0 C\right)_2}$, $M_2=\frac{\mu_0 K_m^2 Ta}{\left(1+\chi_m\right)\left(\rho_0 C\right)_2}$ and $G=\frac{\tau\kappa}{2d^2}$.

Taking $M_2=0$ (see Finlayson [3]) and $\lambda=1$, we have the following

$$\begin{aligned} &\left(1+F_1\,\sigma\right)\left[\frac{\sigma}{\mathrm{Pr}}\left(D^2-a^2\right)W+\left(R+N\right)a^2\,\Theta-N\,a^2\,D\Phi\right] \\ &=\left(1+F_2\,\sigma\right)\left[-Da^{-1}\left(\frac{1}{\xi}D^2-a^2\right)W+\Lambda\left(D^2-a^2\right)^2 W\right] \end{aligned} \tag{3.17}$$

$$\left(1+2G\sigma\right)\left(\sigma\Theta-W\right)=\left(D^2-\eta a^2\right)\Theta-G\left(D^2-a^2\right)W \tag{3.18}$$

$$\left(D^2-M_3\,a^2\right)\Phi-D\Theta=0 \tag{3.19}$$

where $F_1 = \dfrac{\lambda_1 \kappa}{d^2}$ is the stress relaxation parameter, $F_2 = \dfrac{\lambda_2 \kappa}{d^2}$ is the strain retardation parameter, $\Pr = \dfrac{\varepsilon \mu_f}{\rho_0 \kappa}$ is the Prandtl number, $R = \dfrac{\rho_0 \alpha g \beta d^4}{\mu_f \kappa}$ is the thermal Rayleigh number, $N = \dfrac{\mu_0 K^2 \beta^2 d^4}{\mu_f (1+\chi_m)\kappa}$ is the magnetic Rayleigh number, $Da^{-1} = \dfrac{d^2}{k}$ is the inverse Darcy number, $\Lambda = \dfrac{\overline{\mu_f}}{\mu_f}$ is the Brinkman number, $G = \dfrac{\tau \kappa}{2d^2}$ is the Cattaneo number, and $M_3 = \dfrac{1+\dfrac{M_0}{H_0}}{1+\chi_m}$ is the non-buoyancy magnetization parameter.

The boundary conditions encompassing free and isothermal surfaces are (see Finlayson [3])

$$W = D^2 W = \Theta = D\Phi = 0 \text{ at } z = \pm 1/2 .$$

3.1 Stationary Instability

In stationary mode equations (3.17) - (3.19) turn out to be the following

$$\Lambda \left(D^2 - a^2\right)^2 W - Da^{-1}\left(\frac{1}{\xi} D^2 - a^2\right) W - (R+N)\, a^2\, \Theta + N\, a^2\, D\Phi = 0 \tag{3.20}$$

$$\left[G\left(D^2 - a^2\right) - 1\right] W - \left(D^2 - \eta a^2\right) \Theta = 0 \tag{3.21}$$

$$\left(D^2 - M_3 a^2\right) \Phi - D\Theta = 0 . \tag{3.22}$$

Equations (3.20) through (3.22) along with the boundary conditions constitute an eigenvalue problem with the thermal Rayleigh number *R* being an eigenvalue. The straightforward solution $W = A_1 \cos(\pi z)$, $\Theta = A_2 \cos(\pi z)$, $\Phi = \dfrac{A_3}{\pi} \sin(\pi z)$, with A_1, A_2 and A_3 being constants, is taken into consideration. On applying the solvability condition, we obtain

$$R^{st} = \frac{\left(\pi^2 + \eta a^2\right)\left[Da^{-1}\left(\pi^2 + a^2 \xi\right) + \left(\pi^2 + a^2\right)^2 \Lambda \xi\right]}{a^2 \xi \left[1 + G\left(\pi^2 + a^2\right)\right]} - \frac{N M_3 a^2}{\left(M_3 a^2 + \pi^2\right)} \tag{3.23}$$

where the superscript '*st*' stands for stationary instability. If $\xi = 1$ and $\eta = 1$, then equation (3.23) exactly coincides with that obtained by Naseer Ahmed et al. [60]. Further, if $M_3 = 0,\ g = 0,\ \Lambda = 0$ and $Da^{-1} = 1$, equation (3.23) reduces to that obtained by Malashetty and Mahantesh Swamy [54].

3.2 Oscillatory Instability

Dimensionless equations associated with the overstable motion (oscillatory instability) are

$$\left[\left(1+F_1\sigma\right)\frac{\sigma}{\mathrm{Pr}} + \left(1+F_2\sigma\right)\left\{Da^{-1}\left(\frac{\pi^2}{\xi}+a^2\right)+\Lambda\left(\pi^2+a^2\right)\right\}\right]\left(\pi^2+a^2\right)A_1 - \left(1+F_1\sigma\right)\left(R+N\right)a^2\ A_2 + \left(1+F_1\sigma\right)Na^2\ A_3 = 0 \tag{3.24}$$

$$\left[1+2G\sigma+G\left(\pi^2+a^2\right)\right]A_1 - \left[\left(\pi^2+\eta a^2\right)+\left(1+2G\sigma\right)\sigma\right]A_2 = 0 \tag{3.25}$$

$$\pi^2 A_2 - \left(\pi^2 + M_3 a^2\right)A_3 = 0\,. \tag{3.26}$$

On applying the solvability condition, we obtain

$$R = \left\{\frac{\left(\pi^2+a^2\eta+\sigma+2G\sigma^2\right)\left(1+F_2\sigma\right)\mathrm{Pr}\left[Da^{-1}\left(\pi^2+a^2\xi\right)+p^2\Lambda\xi\right]+p\xi\sigma\left(1+F_1\sigma\right)}{a^2\,\mathrm{Pr}\,\xi\left(1+F_1\sigma\right)\left[1+G\left(p+2\sigma\right)\right]}\right\} - \frac{NM_3a^2}{M_3a^2+\pi^2} \tag{3.27}$$

where $p = \pi^2 + a^2$. Introducing the frequency of oscillation ω through $\sigma = i\omega$ and since the Rayleigh number *R* cannot be imaginary, we obtain *R* in the form $R = R_1 + iR_2$. Both R_1 and R_2 are computed by means of the sophisticated MATHEMATICA application package.

4. RESULTS AND DISCUSSION

The study is concerned with anisotropic porous medium viscoelastic ferromagnetic instability with heat conduction law due to Maxwell-Cattaneo. An analytical solution to the subsequent eigenvalue problem, encompassing stationary and oscillatory convection, is obtained by embracing simplified boundary conditions. The thermal Rayleigh number *R*, characterising the stability of the system, is obtained as a function of the different parameters of the study. The mathematical application package MATHEMATICA is used to determine the eigenvalue expressions and the associated critical numbers. Stationary Rayleigh number R^{st} is independent of viscoelastic parameter as seen from the expression (3.23). Hence, as for the stationary convection, viscoelastic fluid behaves the same as the Newtonian fluid. Rayleigh number for oscillatory mode is obtained as a function of the viscoelastic parameters, namely, stress relaxation time and strain retardation time,

Prandtl number, Cattaneo number, non-buoyancy-magnetization parameter, magnetic Rayleigh number, Brinkman number, inverse Darcy number, mechanical and thermal anisotropic parameters. As for the range of values of the different parameters used in the study, it should be mentioned that only experimentally relevant values are considered in the study.

In Fig. 2 critical Rayleigh number R_c is expressed as a function of magnetic Rayleigh number N by keeping all other parameters fixed. As N increases, R_c decreases and hence the system gets destabilized. We observe that oscillatory convection is preferred to stationary convection as R_c^{osc} is very much less than R_c^{st} and hence the principle of exchange of instabilities (PES) is invalid for the problem at hand. Table 1 also settles that the preferred mode of instability is oscillatory rather than stationary.

In Fig. 3 critical oscillatory Rayleigh number R_c^{osc} is expressed as a function of magnetic Rayleigh number N by varying F_1 and keeping all other parameters fixed. We notice that, as F_1 increases, R_c^{osc} value decreases which indicates that the stress relaxation parameter F_1 hastens the oscillatory convection. Hence the system gets destabilized due to the stress relaxation component.

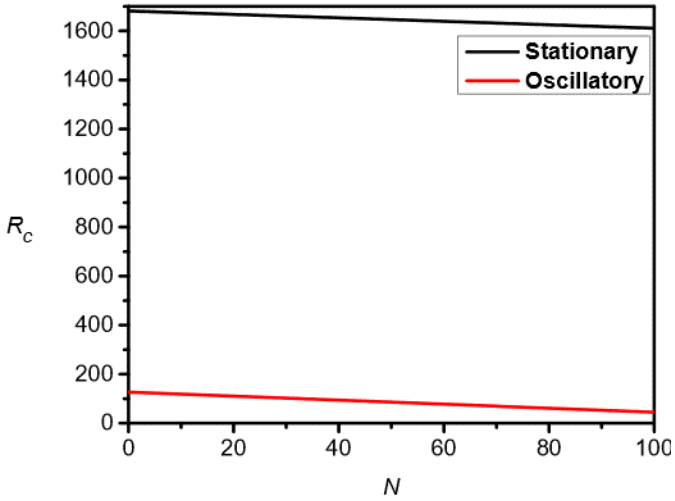

Figure 2. Plot of R_c versus N with

$F_1 = 1.5,\ F_2 = 0.3,\ \mathrm{Pr} = 10,\ Da^{-1} = 5,\ \Lambda = 3,\ G = 0.06,\ M_3 = 3,\ \xi = 0.5\ and\ \eta = 0.3.$

In Fig. 4 critical oscillatory Rayleigh number R_c^{osc} is expressed as a function of the magnetic Rayleigh number N by varying F_2 and keeping all other parameters fixed. As there is an increase in the values of F_2 , we notice that there is an increment in R_c^{osc} , which indicates that the strain retardation parameter F_2 slows down the onset of oscillatory ferroconvection.

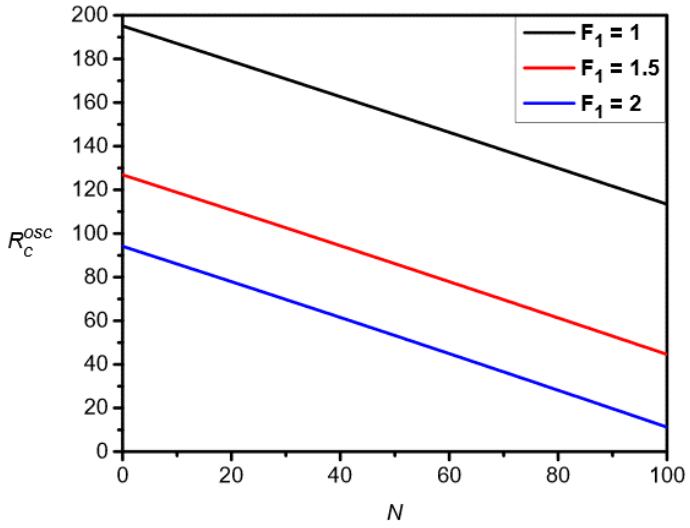

Figure 3. Plot of R_c^{osc} versus N with variation in F_1 and with $F_2 = 0.3$, $\mathrm{Pr} = 10$, $Da^{-1} = 5$, $\Lambda = 3$, $G = 0.06$, $M_3 = 3$, $\xi = 0.5$ *and* $\eta = 0.3$

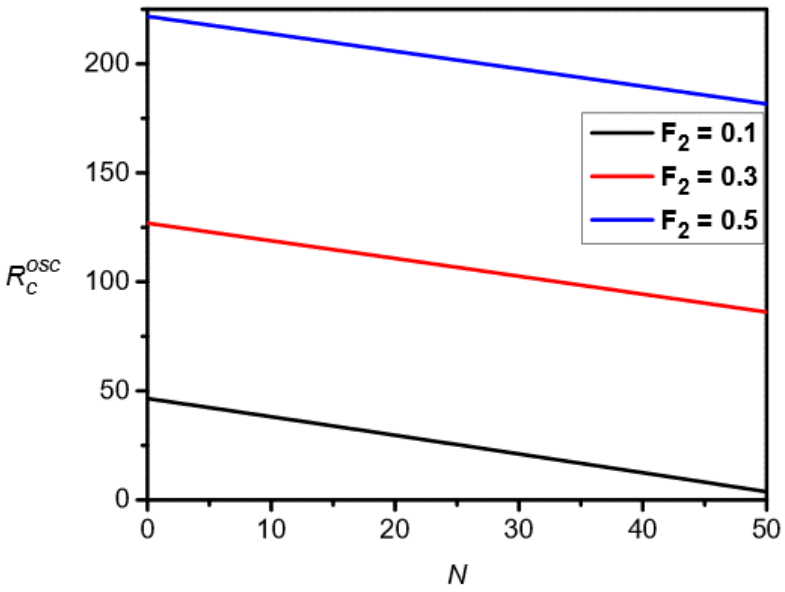

Figure 4. Plot of R_c^{osc} versus N with variation in F_2 and with $F_1 = 1.5$, $\mathrm{Pr} = 10$, $Da^{-1} = 5$, $\Lambda = 3$, $G = 0.06$, $M_3 = 3$, $\xi = 0.5$ *and* $\eta = 0.3$

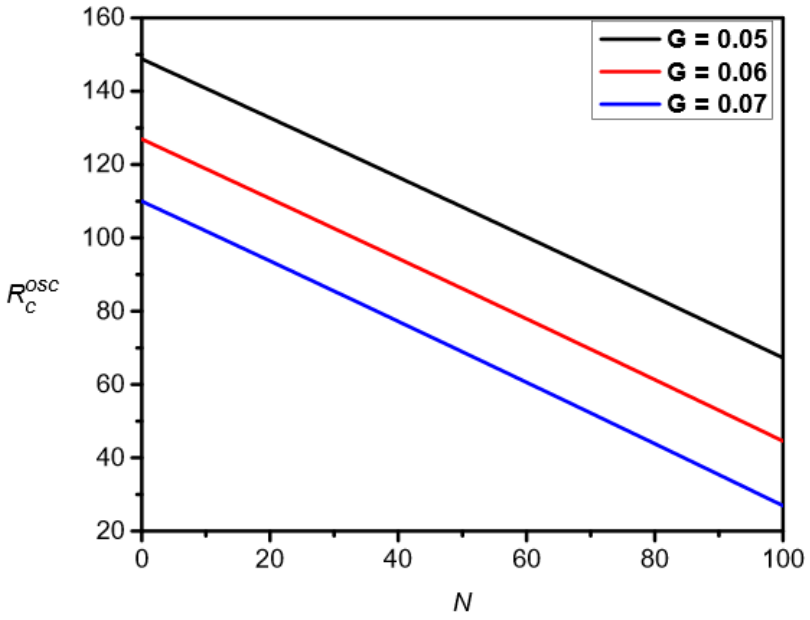

Figure 5. Plot of R_c^{osc} versus N with variation in G and with

$F_1=1.5,\ F_2=0.3,\ \mathrm{Pr}=10,\ Da^{-1}=5,\ \Lambda=3,\ M_3=3,\ \xi=0.5\ and\ \eta=0.3$

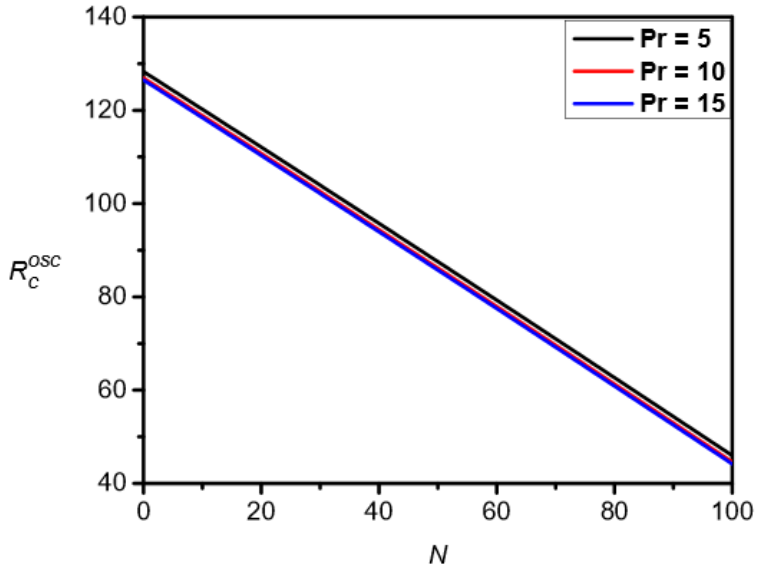

Figure 6. Plot of R_c^{osc} versus N with variation in Pr and with

$F_1=1.5,\ F_2=0.3,\ Da^{-1}=5,\ \Lambda=3,\ G=0.06,\ M_3=3,\ \xi=0.5\ and\ \eta=0.3$

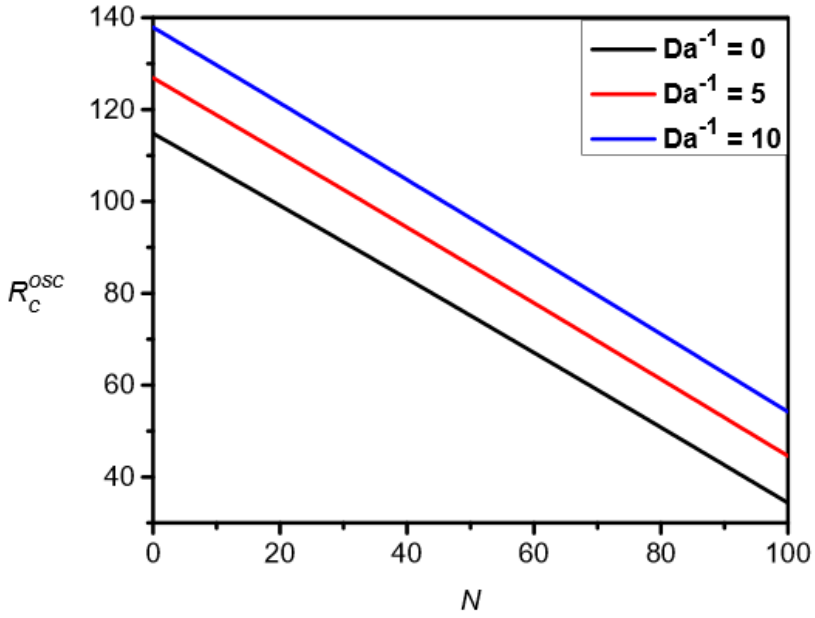

Figure 7. Plot of R_c^{osc} versus N with variation in Da^{-1} and with $F_1 = 1.5,\ F_2 = 0.3,\ \mathrm{Pr} = 10,\ \Lambda = 3,\ G = 0.06,\ M_3 = 3,\ \xi = 0.5$ *and* $\eta = 0.3$

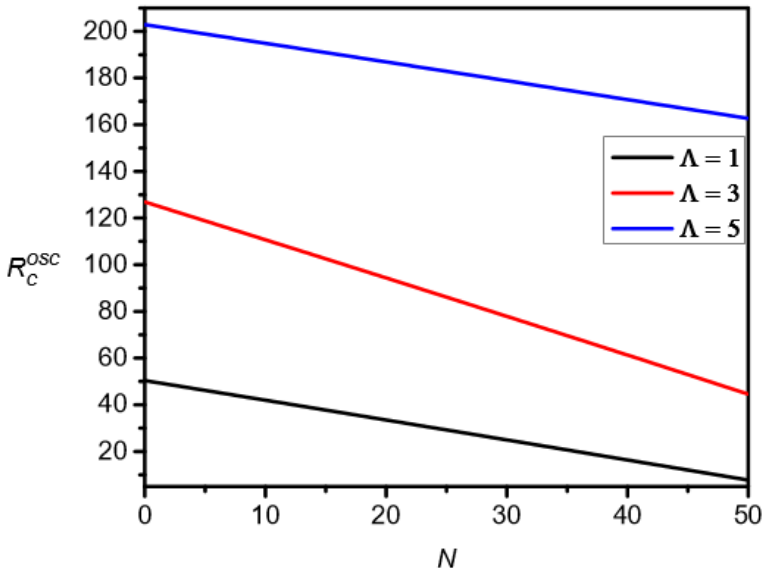

Figure 8. Plot of R_c^{osc} versus N with variation in Λ and with $F_1 = 1.5,\ F_2 = 0.3,\ \mathrm{Pr} = 10,\ Da^{-1} = 5,\ G = 0.06\ M_3 = 3\ \xi = 0.5$ *and* $\eta = 0.3$

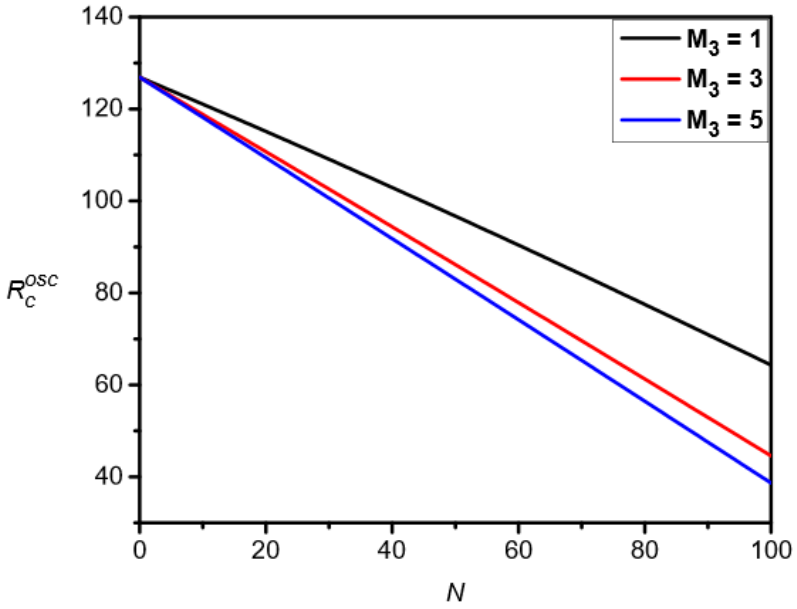

Figure 9. Plot of R_c^{osc} versus N with variation in M_3 and with

$F_1 = 1.5,\ F_2 = 0.3,\ \mathrm{Pr} = 10,\ Da^{-1} = 5,\ \Lambda = 3,\ G = 0.06,\ \xi = 0.5\ and\ \eta = 0.3$

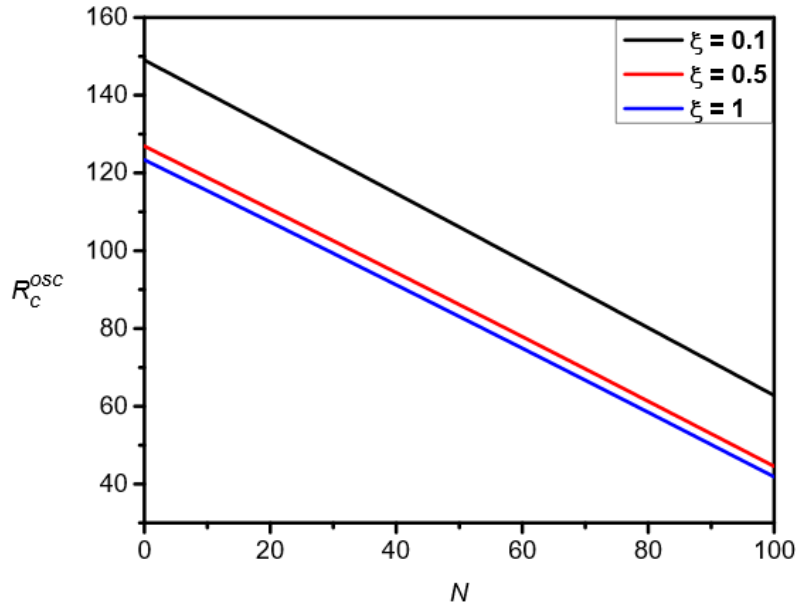

Figure 10. Plot of R_c^{osc} versus N with variation in ξ and with

$F_1 = 1.5,\ F_2 = 0.3,\ \mathrm{Pr} = 10,\ Da^{-1} = 5,\ \Lambda = 3,\ G = 0.06,\ M_3 = 3,\ and\ \eta = 0.3$

In Fig. 5 critical oscillatory Rayleigh number R_c^{osc} is expressed as a function of the magnetic Rayleigh number N by varying the Cattaneo number G and keeping all other parameters fixed.

Evidently, R_c^{osc} decreases with an increase in G, which indicates that the second sound mechanism accelerates oscillatory ferroconvection and hence the system get destabilized.

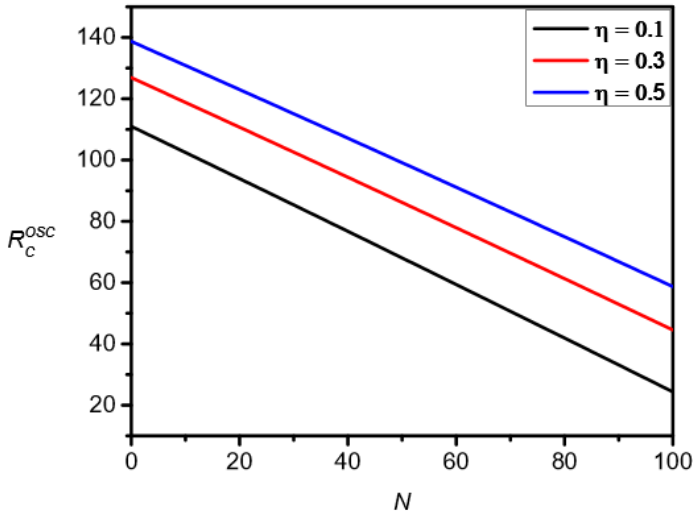

Figure 11. Plot of R_c^{osc} versus N with variation in η and with

$$F_1 = 1.5,\ F_2 = 0.3,\ \mathrm{Pr} = 10,\ Da^{-1} = 5,\ \Lambda = 3,\ G = 0.06,\ M_3 = 3,\ and\ \xi = 0.5$$

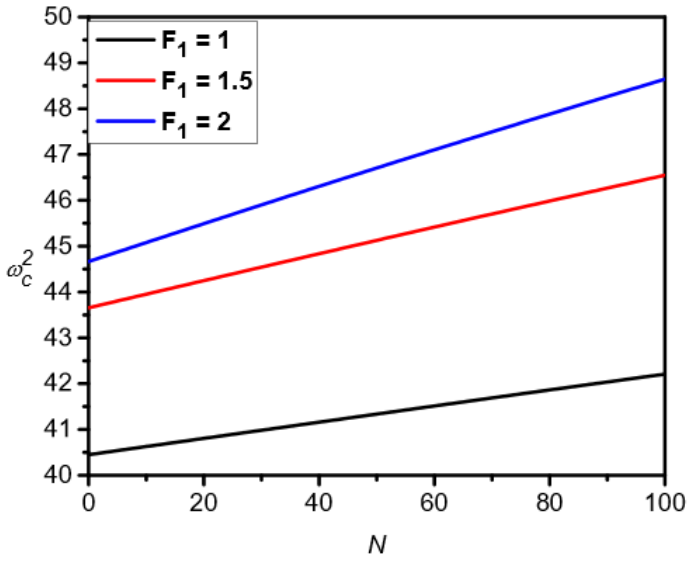

Figure 12. Plot of ω_c^2 versus N with variation in F_1 and with

$$F_2 = 0.3,\ \mathrm{Pr} = 10,\ Da^{-1} = 5,\ \Lambda = 3,\ G = 0.06,\ M_3 = 3,\ \xi = 0.5\ and\ \eta = 0.3$$

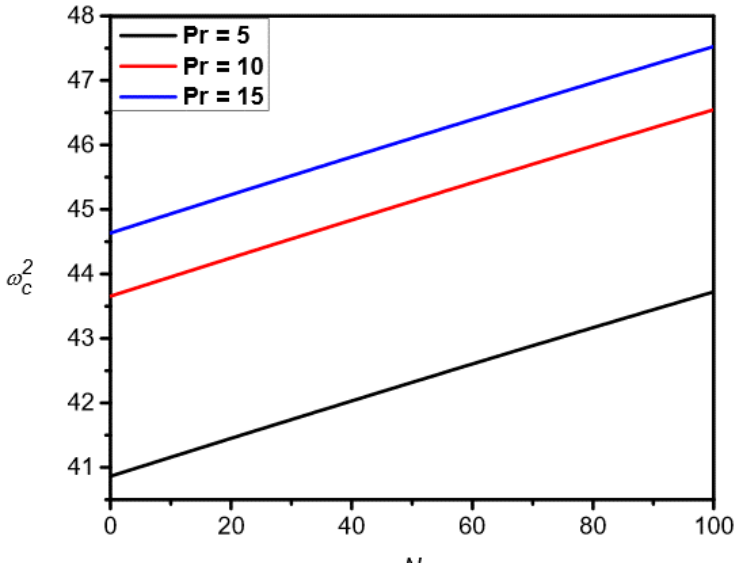

Figure 13. Plot of ω_c^2 versus N with variation in Pr and with $F_1=1.5,\ F_2=0.3,\ Da^{-1}=5,\ \Lambda=3,\ G=0.06,\ M_3=3,\ \xi=0.5\ and\ \eta=0.3$

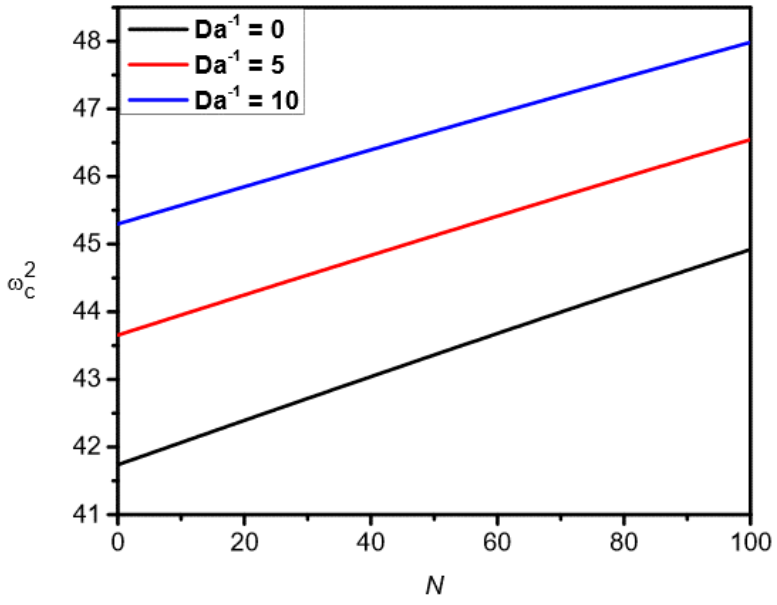

Figure 14. Plot of ω_c^2 versus N with variation in Da^{-1} and with $F_1=1.5,\ F_2=0.3,\ \mathrm{Pr}=10,\ \Lambda=3,\ G=0.06,\ M_3=3,\ \xi=0.5\ and\ \eta=0.3$

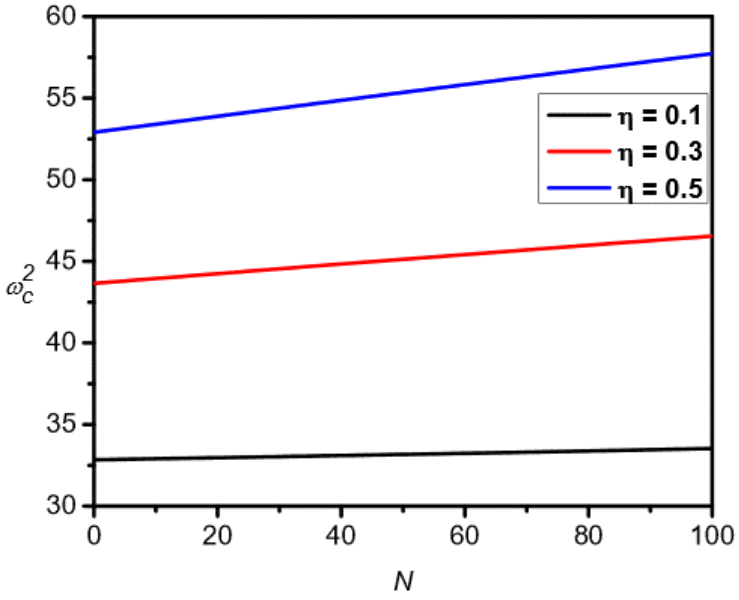

Figure 15. Plot of ω_c^2 versus N with variation in η and with

$F_1 = 1.5,\ F_2 = 0.3,\ \mathrm{Pr} = 10,\ Da^{-1} = 5,\ \Lambda = 3,\ G = 0.06,\ M_3 = 3,\ and\ \xi = 0.5$

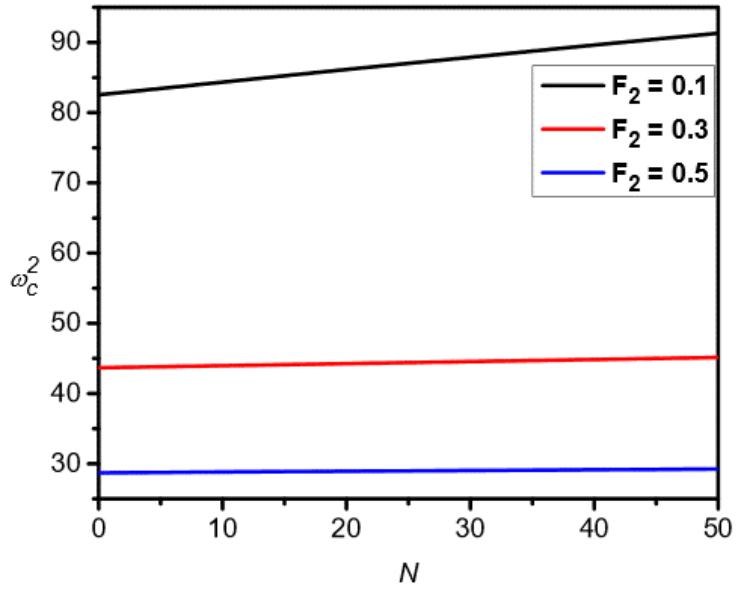

Figure 16. Plot of ω_c^2 versus N with variation in F_2 and with

$F_1 = 1.5,\ \mathrm{Pr} = 10,\ Da^{-1} = 5,\ \Lambda = 3,\ G = 0.06,\ M_3 = 3,\ \xi = 0.5\ and\ \eta = 0.3$

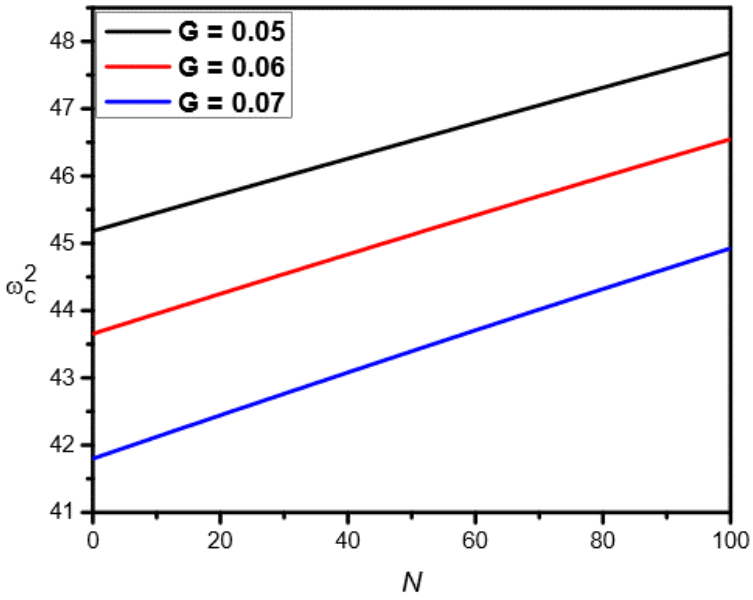

Figure 17. Plot of ω_c^2 versus N with variation in G and with

$F_1=1.5,\ F_2=0.3,\ \mathrm{Pr}=10, Da^{-1}=5,\ \Lambda=3,\ M_3=3,\ \xi=0.5\ and\ \eta=0.3$

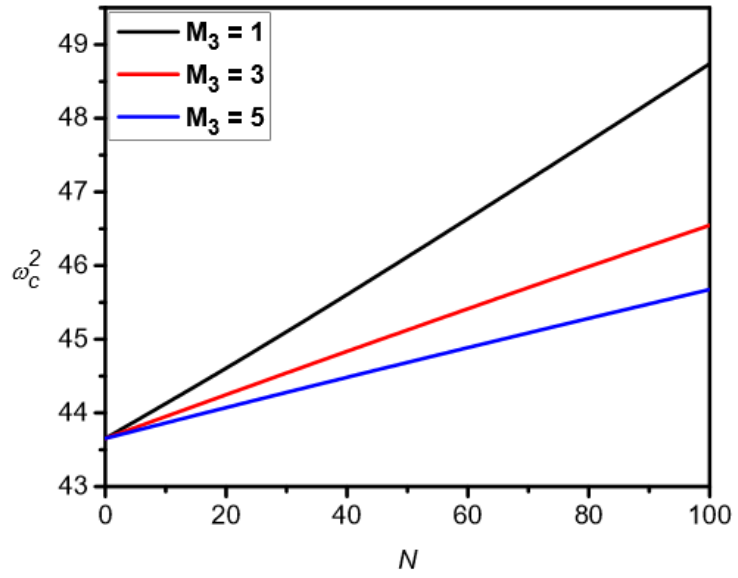

Figure 18. Plot of ω_c^2 versus N with variation in M_3 and with

$F_1=1.5,\ F_2=0.3,\ \mathrm{Pr}=10, Da^{-1}=5,\ \Lambda=3,\ G=0.06,\ \xi=0.5\ and\ \eta=0.3$

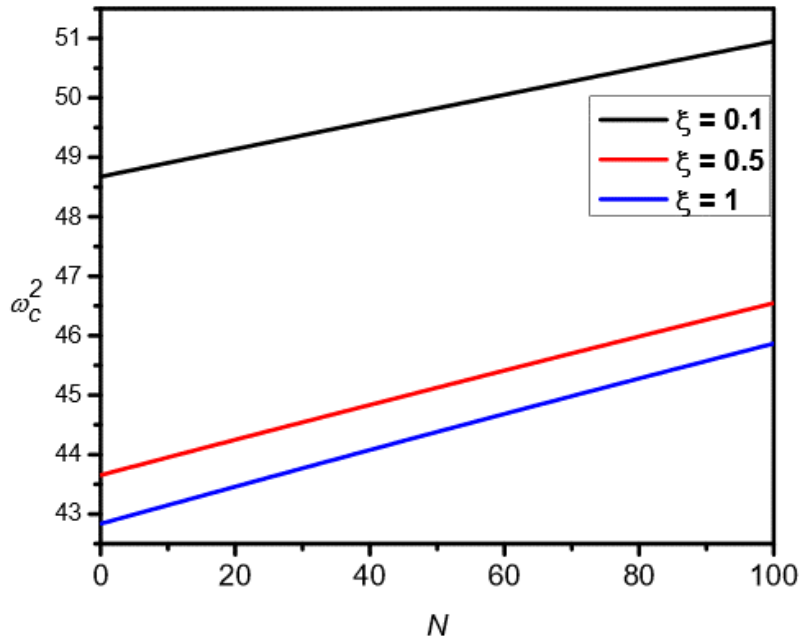

Figure 19. Plot of ω_c^2 versus N with variation in ξ and with

$F_1=1.5,\ F_2=0.3,\ \mathrm{Pr}=10,\ Da^{-1}=5,\ \Lambda=3,\ G=0.06,\ M_3=3\ and\ \eta=0.3$

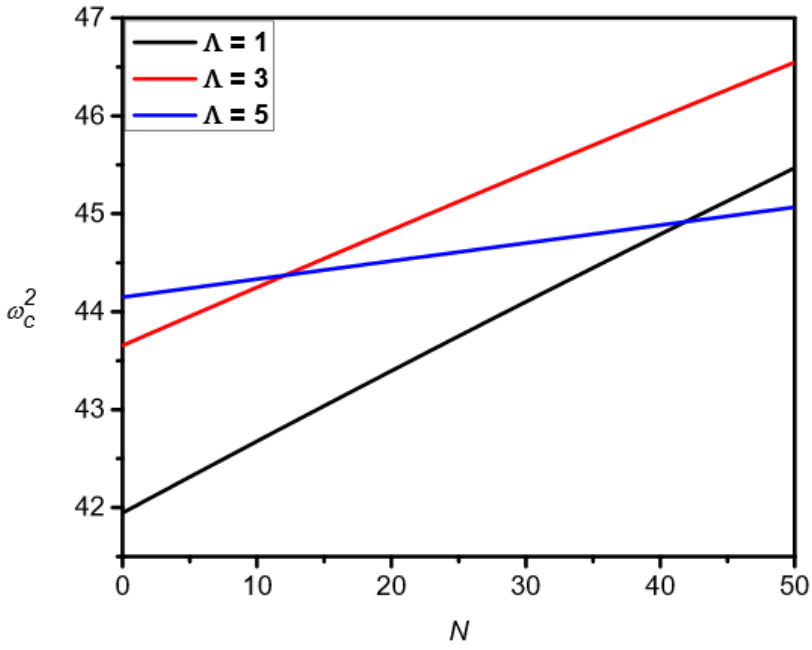

Figure 20. Plot of ω_c^2 versus N with variation in Λ and with

$F_1=1.5,\ F_2=0.3,\ \mathrm{Pr}=10,\ Da^{-1}=5,\ G=0.06,\ M_3=3,\ \xi=0.5\ and\ \eta=0.3$

Stationary vs Oscillatory Instability

Table 1. Critical values of the Rayleigh number and wave number by fixing $F_1 = 1.5,\ F_2 = 0.3,\ \mathrm{Pr} = 10,\ Da^{-1} = 5,\ \Lambda = 3,\ G = 0.06, M_3 = 3,\ \xi = 0.5$ *and* $\eta = 0.3$

N	**Stationary**		**Oscillatory**	
	R_c^{st}	α_c^{st}	R_c^{osc}	α_c^{osc}
0	1681.7	2.79785	126.911	3.69237
20	1667.61	2.80316	110.719	3.78829
40	1653.5	2.80846	94.3753	3.88084
60	1639.38	2.81375	77.8939	3.97005
80	1625.24	2.81902	61.2864	4.056
100	1611.09	2.82428	44.5633	4.13882

Table 2. Critical values of the Rayleigh number and wave number by fixing

$F_2 = 0.3,\ \mathrm{Pr} = 10,\ Da^{-1} = 5,\ \Lambda = 3,\ G = 0.06, M_3 = 3,\ \xi = 0.5$ *and* $\eta = 0.3$

N	$F_1 = 1$		$F_1 = 1.5$		$F_1 = 2$	
	R_c^{osc}	α_c	R_c^{osc}	α_c	R_c^{osc}	α_c
0	195.126	3.68632	126.911	3.69237	94.1353	3.69256
20	178.971	3.74895	110.719	3.78829	77.9158	3.8212
40	162.715	3.81016	94.3753	3.88084	61.4986	3.94372
60	146.363	3.86995	77.8939	3.97005	44.9066	4.06025
80	129.921	3.92833	61.2864	4.056	28.159	4.1711
100	113.394	3.98531	44.5633	4.13882	11.2726	4.27661

Table 3. Critical values of the Rayleigh number and wave number by fixing

$F_1 = 1.5,\ \mathrm{Pr} = 10,\ Da^{-1} = 5,\ \Lambda = 3,\ G = 0.06, M_3 = 3,\ \xi = 0.5$ *and* $\eta = 0.3$

N	$F_2 = 0.1$		$F_2 = 0.3$		$F_2 = 0.5$	
	R_c^{osc}	α_c	R_c^{osc}	α_c	R_c^{osc}	α_c
0	46.5229	4.05473	126.911	3.69237	221.76	3.60605
10	38.1389	4.20799	118.835	3.74075	213.767	3.63308
20	29.6607	4.35403	110.719	3.78829	205.751	3.65984
30	21.0999	4.49303	102.565	3.83499	197.711	3.68633
40	12.4663	4.62529	94.3753	3.88084	189.649	3.71255
50	3.76813	4.75122	86.1511	3.92586	181.565	3.73851

Table 4. Critical values of the Rayleigh number and wave number by fixing

$F_1 = 1.5,\ F_2 = 0.3,\ Da^{-1} = 5,\ \Lambda = 3,\ G = 0.06, M_3 = 3,\ \xi = 0.5$ *and* $\eta = 0.3$

N	$\mathrm{Pr} = 5$		$\mathrm{Pr} = 10$		$\mathrm{Pr} = 15$	
	R_c^{osc}	α_c	R_c^{osc}	α_c	R_c^{osc}	α_c
0	128.291	3.69016	126.911	3.69237	126.488	3.69417
20	112.104	3.78493	110.719	3.78829	110.292	3.79044
40	95.7663	3.8764	94.3753	3.88084	93.9454	3.88332
60	79.2923	3.9646	77.8939	3.97005	77.4602	3.97282
80	62.6931	4.04962	61.2864	4.056	60.8486	4.05905
100	45.9791	4.13157	44.5633	4.13882	44.1212	4.14212

Table 5. Critical values of the Rayleigh number and wave number by fixing

$F_1 = 1.5,\ F_2 = 0.3,\ \mathrm{Pr} = 10,\ \Lambda = 3,\ G = 0.06, M_3 = 3,\ \xi = 0.5$ *and* $\eta = 0.3$

N	$Da^{-1} = 0$		$Da^{-1} = 5$		$Da^{-1} = 10$	
	R_c^{osc}	α_c	R_c^{osc}	α_c	R_c^{osc}	α_c
0	114.822	3.42152	126.911	3.69237	137.938	3.91789
20	99.1002	3.53274	110.719	3.78829	121.405	4.00296
40	83.174	3.63965	94.3753	3.88084	104.754	4.08503
60	67.0643	3.74218	77.8939	3.97005	87.9946	4.16496
80	50.7891	3.8404	61.2864	4.05600	71.1338	4.24203
100	34.3644	3.93447	44.5633	4.13882	54.1795	4.31659

Table 6. Critical values of the Rayleigh number and wave number by fixing

$F_1 = 1.5,\ F_2 = 0.3,\ \mathrm{Pr} = 10,\ Da^{-1} = 5,\ G = 0.06, M_3 = 3,\ \xi = 0.5$ *and* $\eta = 0.3$

N	$\Lambda = 1$		$\Lambda = 3$		$\Lambda = 5$	
	R_c^{osc}	α_c	R_c^{osc}	α_c	R_c^{osc}	α_c
0	50.3609	4.0999	126.911	3.69237	202.872	3.59234
10	41.9608	4.21214	110.719	3.78829	194.889	3.62327
20	33.4918	4.31952	94.3753	3.88084	186.88	3.65388
30	24.9607	4.42225	77.8939	3.97005	178.844	3.68415
40	16.3736	4.52058	61.2864	4.056	170.782	3.71408
50	7.73562	4.6148	44.5633	4.13882	162.695	3.74368

Table 7. Critical values of the Rayleigh number & wave number by fixing

$F_1 = 1.5,\ F_2 = 0.3,\ \mathrm{Pr} = 10,\ Da^{-1} = 5,\ \Lambda = 3, M_3 = 3,\ \xi = 0.5$ *and* $\eta = 0.3$

N	$G = 0.05$		$G = 0.06$		$G = 0.07$	
	R_c^{osc}	α_c	R_c^{osc}	α_c	R_c^{osc}	α_c
10	148.78	3.61641	126.911	3.69237	109.986	3.75667
20	132.729	3.69701	110.719	3.78829	93.6768	3.86861
40	116.543	3.77522	94.3753	3.88084	77.2001	3.97595
60	100.233	3.85106	77.8939	3.97005	60.5725	4.07877
80	83.8084	3.92454	61.2864	4.056	43.8088	4.17725
100	67.2763	3.99574	44.5633	4.13882	26.9217	4.2716

Table 8. Critical values of the Rayleigh number and wave number by fixing

$F_1 = 1.5,\ F_2 = 0.3,\ \mathrm{Pr} = 10,\ Da^{-1} = 5,\ \Lambda = 3,\ G = 0.06,\ \xi = 0.5$ *and* $\eta = 0.3$

N	$M_3 = 1$		$M_3 = 3$		$M_3 = 5$	
	R_c^{osc}	α_c	R_c^{osc}	α_c	R_c^{osc}	α_c
0	126.911	3.69237	126.911	3.69237	126.911	3.69237
20	115.112	3.84538	110.719	3.78829	109.4	3.76006
40	102.929	3.99925	94.3753	3.88084	91.8136	3.8255
60	90.3837	4.15188	77.8939	3.97005	74.1562	3.88881
80	77.5008	4.30165	61.2864	4.056	56.4334	3.95007
100	64.306	4.44739	44.5633	4.13882	38.6497	4.00942

Table 9. Critical values of the Rayleigh number and wave number by fixing $F_1 = 1.5,\ F_2 = 0.3,\ \mathrm{Pr} = 10,\ Da^{-1} = 5,\ \Lambda = 3,\ G = 0.06, M_3 = 3,\ and\ \eta = 0.3$

N	$\xi = 0.1$		$\xi = 0.5$		$\xi = 1$	
	R_c^{osc}	α_c	R_c^{osc}	α_c	R_c^{osc}	α_c
0	149.04	4.38876	126.911	3.69237	123.388	3.57071
20	131.922	4.45375	110.719	3.78829	107.398	3.6737
40	114.732	4.51714	94.3753	3.88084	91.2337	3.77286
60	97.4767	4.57898	77.8939	3.97005	74.9122	3.86818
80	80.1585	4.6393	61.2864	4.056	58.4479	3.95976
100	62.7812	4.69817	44.5633	4.13882	41.8534	4.04774

Table 10. Critical values of the Rayleigh number and wave number by fixing $F_1 = 1.5,\ F_2 = 0.3,\ \mathrm{Pr} = 10,\ Da^{-1} = 5,\ \Lambda = 3,\ G = 0.06, M_3 = 3\ and\ \xi = 0.5$

N	$\eta = 0.1$		$\eta = 0.3$		$\eta = 0.5$	
	R_c^{osc}	α_c	R_c^{osc}	α_c	R_c^{osc}	α_c
0	110.976	4.29341	126.911	3.69237	138.727	3.43864
20	93.9227	4.43406	110.719	3.78829	123.001	3.52043
40	76.716	4.56935	94.3753	3.88084	107.122	3.59967
60	59.3726	4.69931	77.8939	3.97005	91.1037	3.67633
80	41.9068	4.82411	61.2864	4.056	74.9561	3.75046
100	24.3307	4.94396	44.5633	4.13882	58.689	3.82211

In Fig. 6 critical oscillatory Rayleigh number R_c^{osc} is expressed as a function of the magnetic Rayleigh number N by varying the Prandtl number Pr and keeping all other parameters fixed. As can be seen, R_c^{osc} decreases with an increase in Pr which indicates that the effect of Prandtl number Pr is to accelerate oscillatory ferroconvection and hence the system is destabilized. In Fig. 7

critical oscillatory Rayleigh number R_c^{osc} is expressed as a function of the magnetic Rayleigh number N by varying Da^{-1} and keeping all other parameters fixed. It is evident that oscillatory ferroconvection is delayed because as Da^{-1} is increased, there is an increase in the values of R_c^{osc}. The reason for this is that an increase in Da^{-1} will result in a decrease in the porous medium permeability and hence the convective instability is impeded.

In Fig. 8 critical oscillatory Rayleigh number R_c^{osc} is expressed as a function of the magnetic Rayleigh number N by varying the Brinkman number Λ and keeping all other parameters fixed. As the Brinkman number Λ increases, R_c^{osc} also increases and therefore oscillatory ferroconvection is delayed. As the Brinkman model accounts for an effective viscosity $\overline{\mu_f}$ which is different from the fluid viscosity μ_f and the ratio is assigned as the Brinkman number. Hence viscous effect increases on increasing the Brinkman number and hence ferroconvective instability is hampered due to the presence of the permeable structure.

In Fig. 9 critical oscillatory Rayleigh number R_c^{osc} is expressed as a function of magnetic Rayleigh number N by varying the non-buoyancy magnetization parameter M_3 and keeping all other parameters fixed. The departure from linearity through the magnetic equation of state is taken care of by the parameter M_3. We notice from Fig. 9 that, as M_3 increases, R_c^{osc} monotonically decreases which implies that magnetic equation of state grows more and more to a nonlinear state due to which ferroconvection is hastened. In Fig. 10 critical oscillatory Rayleigh number R_c^{osc} is expressed as a function of the magnetic Rayleigh number N by varying the mechanical anisotropy parameter ξ and keeping all other parameters fixed. It is observed that R_c^{osc} decreases with an increase in ξ which indicates that the effect of ξ is to hasten the oscillatory ferroconvection. The reason being that, as ξ increases, the horizontal permeability increases which eases the fluid flow in that direction, so conduction becomes more unsettled and hence instability is triggered.

In Fig. 11 critical oscillatory Rayleigh number R_c^{osc} is expressed as a function of the magnetic Rayleigh number N by varying the thermal anisotropy parameter η and keeping all other parameters fixed. Clearly ferroconvection onset is delayed due to the presence of the thermal anisotropy. The reason for this delayed ferroconvection is that as η increases in the horizontal direction less heat is lost by the heated fluid, so its buoyancy is maintained better. From Figs. 12 through 15, one can observe that when all the respective parameters increase, ω_c^2 also increases, whereas from Figs. 16 through 19, as all the parameters concerned increase, ω_c^2 decreases. But in Fig. 20 we can observe that ω_c^2 intersects as Λ increases. Hence, we can conclude from Figs. 12 through 20 that the frequency of oscillatory ferroconvective instability is sensitive to all the parameters of the study. On the other hand, wave number depicts the size and shape of the convection cell. From Tables 2 through 10, it follows that ferroconvection cell size is also sensitive to the all the parameters of the study at hand. Indeed, the convection cell size is enlarged with an increase in F_2, Λ, M_3, ξ and η, and the opposite is found to be true with respect to an increase in the rest of the parameters.

5. CONCLUSIONS

1. The system is destabilized through the presence of magnetic forces caused by the magnetization of ferrofluids.
2. Nonlinearity in magnetization is shown to destabilize the system.
3. Viscoelastic relaxation, Prandtl number, Cattaneo number and mechanical anisotropy parameter are shown to destabilize the system.

4. Viscoelastic retardation, inverse Darcy number, Brinkman and thermal anisotropic parameter are shown to stabilize the system.
5. Critical wave number and frequency of oscillatory motion are calculated as functions of all the parameters arising in the study. Both critical wave number and frequency of oscillatory motion are shown to be sensitive to all the parameters of the problem.

6. REFERENCES

1. M. T. Shliomis, "Magnetic fluids", Sov. Phys. Usp., Vol. 17, pp. 153-169, 1974.
2. R. E. Rosensweig, "Ferrohydrodynamics", Cambridge University Press, Cambridge, 1985.
3. B. A. Finlayson, "Convective instability of ferromagnetic fluids", J. Fluid Mech., Vol. 40, pp. 753-167, 1970.
4. L. Schwab, U. Hildebrandt, and K. Stierstadt, "Magnetic Bénard convection," J. Magn. Magn. Mater., Vol. 39, pp. 113-124, 1983.
5. P. J. Stiles and M. J. Kagan, "Thermoconvective instability of a horizontal layer of ferrofluid in a strong vertical magnetic field", J. Magn. Magn. Mater., Vol. 85, pp. 196-198 1990.
6. D. P. Lalas and S. Carmi, "Thermoconvective stability of ferrofluids", Phys. Fluids, Vol. 14, pp. 436-437, 1971.
7. R. Bajaj and S. K. Malik, "Pattern formation in ferrofluids", J. Magn. Magn. Mater., Vol. 149, pp. 158-161, 1995.
8. R. Bajaj and S. K. Malik, "Convective instability and pattern formation in magnetic fluids", J. Math. Anal. Appl., Vol. 207, pp. 172-191, 1997.
9. S. Maruthamanikandan, "Effect of radiation on Rayleigh-Bénard convection in ferromagnetic fluids", Int. J. Appl. Mech. Engg., Vol. 8, pp. 449-459, 2003.
10. B. Straughan, "Ferrohydrodynamic convection", In The Energy Method, Stability, and Nonlinear Convection (Applied Mathematical Sciences, Springer, New York), 2004.
11. S. A. Suslov, "Thermomagnetic convection in a vertical layer of ferromagnetic fluid," Phys. Fluids, Vol. 24, p. 084101, 2008.
12. P. Dey and S. A. Suslov, "Thermomagnetic instabilities in a vertical layer of ferrofluid: Nonlinear analysis away from a critical point," Fluid Dyn. Res., Vol. 48, p. 061404, 2016.
13. A. Mahajan and M. K. Sharma, "Penetrative convection in magnetic nanofluids via internal heating", Phys. Fluids, Vol. 29, p. 034101, 2017.
14. Nisha Mary Thomas and S. Maruthamanikandan, "Gravity modulation effect on ferromagnetic convection in a Darcy-Brinkman layer of porous medium", J. Phys.: Conf. Ser., Vol. 1139 (1), p. 012022, 2018.
15. S. Maruthamanikandan, Nisha Mary Thomas and Soya Mathew, "Thermorheological and magnetorheological effects on Marangoni-ferroconvection with internal heat generation", J. Phys.: Conf. Series, Vol. 1139, p. 012024, 2018.
16. C. Balaji, C. Rudresha, V. Vidya shree and S. maruthamanikandan, "Ferroconvection in a sparsely distributed porous medium with time-dependent sinusoidal magnetic field", J. Mines, Metals and Fuels, Vol. 70 (3A), pp.28-34, 2022.
17. V. Vidya shree, C. Rudresha, C. Balaji and S. Maruthamanikandan, "Effect of MFD viscosity on ferroconvection in a fluid saturated porous medium with variable gravity", J. Mines, Metals and Fuels, Vol. 70 (3A), pp.98-103, 2022.
18. Balaji C, Rudresha C, V. Vidya Shree and S. Maruthamanikandan, "Ferrohydrodynamic instability of a couple stress magnetic fluid layer under the influence of time-dependent sinusoidal magnetic field", Iraqi J. Appl. Phys., Vol. 18 (4), pp. 15-19, 2022.
19. C. W. Horton and F. T. Rogers, "Convection Currents in a Porous Medium", J. Appl. Phys., Vol. 16, pp. 367-370, 1945.
20. E. Lapwood, "Convection of a fluid in a porous medium", In Mathematical Proceedings of the Cambridge Philosophical Society, Vol. 44 (4), pp. 508-521, 1948.

21. M. S. Malashetty and V. Padmavathi, "Effect of gravity modulation on the onset of convection in a fluid and porous layer", Int. J. Engng. Sci., Vol. 35 (9), pp. 829-840, 1997.
22. S. Govender, "Oscillatory convection induced by gravity and centrifugal forces in a rotating porous layer distant from the axis of rotation", Int. J. Engng. Sci., Vol. 41 (6), pp. 539-545, 2003.
23. M. F. El Sayed, "Onset of electroconvective instability of Oldroydian viscoelastic liquid layer in Brinkman porous medium", Arch. Appl. Mech., Vol. 78 (3), pp. 211-224, 2008.
24. A. V. Kuznetsov and D. Nield, "Thermal instability in a porous medium layer saturated by a nanofluid: Brinkman model", Trans. Porous Media, Vol. 81(3), pp. 409-422, 2010.
25. I. A. Eltayeb, "Stability of a porous Bènard-Brinkman layer in local thermal non-equilibrium with Cattaneo effects in solid", Int. J. Thermal Sci., Vol. 98, pp. 208-218, 2015.
26. Soya Mathew and S. Maruthamanikandan, "Darcy-Brinkman Ferroconvection with temperature dependent viscosity", J. Phys.: Conf. Ser., Vol. 1139 (1), pp. 012023-012031, 2018.
27. S. Saravanan and M. Meenasaranya, "Energy stability of modulation driven porous convection with magnetic field", Meccanica, Vol. 56 (11), pp. 2777-2788, 2021.
28. M. Castinel, G. and Combarnous, "Criterion for appearance of natural-convection in horizontal anisotropic porous film", Comptes rendus hebdomadaires des seances de l academie des sciences serie B, Vol. 278 (15), pp. 701-704, 1974.
29. O. Kvernvold and P. A. Tyvand, "Nonlinear thermal convection in anisotropic porous media", J. Fluid Mech., Vol. 90 (4), pp. 609-624, 1979.
30. R. Sekar, G. Vaidyanathan, and A. Ramanathan, "Ferroconvection in an anisotropic porous medium", Int. J. Engng. Sci., Vol. 34 (4), pp. 399-405, 1996.
31. D. A. S. Rees and A. Postelnicu, "The onset of convection in an inclined anisotropic porous layer", Int. J. Heat Mass Trans., Vol. 44 (21), pp. 4127–4138, 2001.
32. S. Govender, "On the effect of anisotropy on the stability of convection in rotating porous media", Trans. Porous Med., Vol. 64 (3), pp. 413-422, 2006.
33. M. S. Malashetty and M. Swamy, "The onset of convection in a viscoelastic liquid saturated anisotropic porous layer", Trans. Porous Med., Vol. 67 (2), pp. 203-218, 2007.
34. M. S. Malashetty and P. Kollur, "The onset of double diffusive convection in a couple stress fluid saturated anisotropic porous layer," Trans. Porous Med., Vol. 86 (2), pp. 435-459, 2011.
35. A. K. Srivastava, B. S. Bhadauria, and V. K. Gupta, "Magneto-convection in an anisotropic porous layer with Soret effect", Int. J. Non-Lin. Mech., Vol. 47 (5), pp. 426-438, 2012.
36. Balaji C, Rudresha C, Vidya Shree V and S. Maruthamanikandan, "Thermomagnetic ferroconvection in an anisotropic permeable layer exposed to a modulated magnetic field", Int. J. Math. Phys., Vol. 13 (2), pp. 58-67, 2022.
37. Rudresha C, Balaji C, Vidya Shree V and S. Maruthamanikandan, "Effect of electric field modulation on the onset of electroconvection in an anisotropic porous layer saturated with a dielectric fluid", J. Comp. Appl. Mech., Vol. 53 (4), pp. 510-523, 2022.
38. B. Straughan and F. Franchi, "Bénard convection and the Cattaneo law for heat conduction", Proc. Royal Soc. Edinburgh: Mathematics, Vol. 96A, pp. 175-178, 1984.
39. B. Straughan, "Oscillatory convection and the Cattaneo law of heat conduction", Ricerche di Matematica, Vol. 58, pp. 157-162, 2009.
40. Soya Mathew and S. Maruthamanikandan, "Oscillatory porous medium ferroconvection with Maxwell-Cattaneo law of heat conduction", J. Phys.: Conf. Ser., Vol. 1850 (1), p. 012024, 2021.
41. Vidya Shree V, Rudresha C, Balaji C and S. Maruthamanikandan, "Effect of magnetic field dependent viscosity on Darcy-Brinkman ferroconvection with second sound", East Eur. J. Phys., Vol. 4, pp. 112-117, 2022.

42. S. Chandrasekhar, "Hydrodynamic and hydromagnetic stability", Oxford University Press, Oxford, 1961.
43. J. K. Platten and J. C. Legros, "Convection in liquids", Springer, Berlin, 1984.
44. R. B. Bird, C. Armstrong and O. Massager, "Dynamics of polymeric liquids", Wiley, New York, 1987.
45. D. D. Joseph, "Fluid dynamics of viscoelastic liquids", Springer, New York, 2013.
46. J. G. Oldroyd, "On the formulation of rheological equations of state", Proc. R. Soc. Lond. A, Vol. 200, pp. 523-541, 1950.
47. C. M. Vest and V. S. Arpaci, "Overstability of a viscoelastic fluid layer heated from below", J. Fluid Mech., Vol. 36, pp. 613-623, 1969.
48. S. F. Liang and A. Acrivos, "Experiments on buoyancy-driven convection in non-Newtonian fluids", Rheol. Acta, Vol. 9, pp. 447-455, 1970.
49. A. V. Shenoy and R. A. Mashelkar, "Thermal convection in non-Newtonian fluids", Adv. Heat Trans., Vol. 15, pp. 143-226, 1982.
50. J. Martınez-Mardones, C. Perez-Garcıa, "Linear instability in viscoelastic fluid convection", J. Phys.: Condens. Matter, Vol. 2, pp. 1281-1290, 1990.
51. P. C. Dauby, P. Parmentier, G. Lebon and M. Grmela, "Coupled buoyancy and thermocapillary convection in a viscoelastic Maxwell fluid", J. Phys. Cond. Matter, Vol. 5, pp. 4343-4352, 1993.
52. G. Lebon, P. Parmentier, O. Teller and P.C. Dauby, "Bénard–Marangoni instability in a viscoelastic Jeffreys' fluid layer", Rheol. Acta, Vol. 33, pp. 257-266, 1994.
53. H. Ramkisoon, G. Ramdath, D. Comissiong and K. Rahaman, "On thermal instabilities in a viscoelastic fluid", Int. J. Non-Lin. Mech., Vol. 41, pp. 18-25, 2006.
54. M. S. Malashetty and Mahantesh Swamy, "The onset of convection in a viscoelastic liquid saturated anisotropic porous layer", Transp. Porous Med., Vol. 67, pp. 203–218, 2007.
55. G. N. Sekhar and G. Jayalatha, "Elastic effects on Rayleigh-Bénard convection in liquids with temperature-dependent viscosity", Int. J. Thermal Sci., Vol. 49, pp. 67-79, 2010.
56. Syeda Khudeja Akbar, S. Maruthamanikandan and Achala L. Nargund, "Convective instability in a horizontal porous layer saturated with a chemically reacting Maxwell fluid", (In the AIP Conference Proceedings: International conference on Mathematical Sciences and Statistics, Kuala Lumpur, Malaysia), Vol. 1557, Issue 1, p. 130, 2013.
57. B. S. Bhadauria and P. Kiran, "Heat and mass transfer for oscillatory convection in a binary viscoelastic fluid layer subjected to temperature modulation at the boundaries", Int. Comm. Heat Mass Trans., Vol. 58, pp. 166-175, 2014.
58. M. N. Mahmud, Z. Siri, J. A. Vélez, L. M. Pérez, and D. Laroze, "Chaotic convection in an Oldroyd viscoelastic fluid in saturated porous medium with feedback control," Chaos: An Interdis. J. Non-Lin. Sci., Vol. 30 (7), pp. 73109-73121, 2020.
59. R. Sharma and P. K. Mondal, "Thermosolutal Marangoni instability in a viscoelastic liquid film: Effect of heating from the free surface", J. Fluid. Mech., Vol. 909, pp. 1-24, 2021.
60. Naseer Ahmed, S. Maruthamanikandan and B. R. Nagasmitha, "Oscillatory porous medium ferroconvection in a viscoelastic magnetic fluid with non-classical heat conduction", East Eur. J. Phys., Vol. 2, pp. 296-309, 2023.